

Sub-Planck-scale structures in a vibrating molecule in the presence of decoherence

Suranjana Ghosh,^{1,*} Utpal Roy,^{1,†} Claudiu Genes,^{2,‡} and David Vitali^{1,§}

¹*Dipartimento di Fisica, Università di Camerino, I-62032 Camerino, Italy*

²*Institute for Theoretical Physics, University of Innsbruck, A-6020 Innsbruck, Austria*

(Received 20 February 2009; published 5 May 2009)

We study the effect of decoherence on the sub-Planck scale structures of the vibrational wave packet of a molecule. The time evolution of these wave packets is investigated under the influence of a photonic or phononic environment. We determine the master equation describing the reduced dynamics of the wave packet and analyze the sensitivity of the sub-Planck structures against decoherence in the case of a hydrogen iodide (HI) molecule.

DOI: [10.1103/PhysRevA.79.052104](https://doi.org/10.1103/PhysRevA.79.052104)

PACS number(s): 03.65.Yz, 42.50.Md, 33.80.-b

I. INTRODUCTION

Recent progress of controlled femtosecond pulses has advanced greatly the technology during the last few years [1]. A new field of molecular optics has emerged where lasers are used to manipulate the internal and external degrees of freedom of molecules, to deflect beams of molecules, to control molecular dynamics, and to align molecules [2,3]. Many investigations have focused on the vibrational motion of diatomic molecules. The single bond between the atoms acts as a spring and supports harmonic oscillations for small amplitudes, but the bond can break (dissociate) when stretched too much. These phenomena usually occur at time scales between few picoseconds and few hundred femtoseconds. With ultrashort pulses one can now prepare a molecular wave packet and probe its evolution and observe molecular reactions in this time domain. Successful experiments have been performed on several molecules [4]. The most convenient model for studying the vibrational motion of diatomic molecule is the Morse potential, which is an exactly solvable system [5]. Coherent superposition of several vibrational levels of the molecule creates the wave packet which, due to quantum interference, shows revival and fractional revivals [6–8] in their time evolution.

Fractional revivals are associated with superpositions of separated wave packets (for example, the so-called Schrödinger cat states), which manifest clear quantum interference effects and nonclassical features, which can be well visualized in the phase space of the vibrational motion. Although the experimental observation of small quantum interference structures is very challenging, it has already been visualized in Pico-meter scale [9]. A number of different phase space distribution functions have been introduced [10] and investigated over the years, and among these the Wigner distribution [11] is particularly useful because its negativity yields an indication of nonclassical behavior [12–14]. Zurek [15] first showed that this negativity reveals the existence of the smallest structures in phase space, i.e., the sub-Planck

scale structures. One may expect that Heisenberg's uncertainty principle implies that structures on scales smaller than the Planck constant have no observable consequence, while instead Zurek [15] showed that these highly nonclassical structures are expected to be particularly sensitive to decoherence. Through a short walk in controversy, recently sub-Planck scale structures draw considerable attention and have been found by others in different situations [16–27].

Decoherence due to the coupling to an external environment is the main responsible for the disappearance of nonclassical manifestations of quantum states and it is considered one of the mechanisms through which the classical world at the macroscopic level emerges from the quantum substrate [28–30]. Decoherence on the molecular vibrational degree of freedom is due to the coupling between vibrational and rotational modes [31] and also to the coupling with the photonic and phononic degrees of freedom [32]. The latter are associated with a super-Ohmic environment describable in terms of a continuous set of bosonic modes and in this paper we shall focus on the effect of this source of decoherence. To be more specific, we will study the sub-Planck scale structures in the Morse system and the effect of decoherence on these structures in molecular wave packets. We shall determine the master equation describing the reduced dynamics of the wave packet and analyze the robustness of the sub-Planck structures against decoherence.

The paper is organized as follows. In Sec. II we give a brief overview of the Morse potential and its coherent states, while in Sec. III we derive the master equation in the case of the coupling with a bosonic environment at thermal equilibrium. In Sec. IV we study the effect of decoherence on the Wigner function at the sub-Planck level and the sensitivity to decoherence of these structures is analyzed. Finally, we conclude in Sec. V.

II. REVIEW OF THE MORSE MODEL OF A VIBRATING MOLECULE

Vibrational dynamics of diatomic molecules are well described by Morse potential [5,33–36]. It can be described as

$$V(x) = D(e^{-2\beta x} - 2e^{-\beta x}), \quad (1)$$

where $x = r/r_0 - 1$, r_0 is the equilibrium value of the internuclear distance r and β is a range parameter. D is the disso-

*suranjana.ghosh@unicam.it

†utpal.roy@unicam.it

‡claudiu.genes@unicam.it

§david.vitali@unicam.it

ciation energy, which has been extensively studied in a wider context of this model [37,38]. Defining

$$\lambda = \sqrt{\frac{2\mu D r_0^2}{\beta^2 \hbar^2}} \quad \text{and} \quad s = \sqrt{-\frac{8\mu r_0^2}{\beta^2 \hbar^2} E}, \quad (2)$$

where μ is the reduced mass of the vibrational motion, the eigenfunctions of the Morse potential can be written as

$$\psi_n^\lambda(\xi) = N e^{-\xi/2} \xi^{s/2} L_n^s(\xi), \quad (3)$$

where $\xi = 2\lambda e^{-\beta x}$, $0 < \xi < \infty$, and $n = 0, 1, \dots, [\lambda - 1/2]$, with $[\rho]$ denoting the integer part of ρ , so that the total number of bound states is $[\lambda - 1/2]$. The parameters λ and s satisfy the constraint condition $s + 2n = 2\lambda - 1$.

Note that λ is potential dependent and s is related to energy E , and, by definition, $\lambda > 0$, $s > 0$. In Eq. (3), $L_n^s(y)$ is the associated Laguerre polynomial and N is the normalization constant,

$$N = \left[\frac{\beta(2\lambda - 2n - 1)\Gamma(n+1)}{\Gamma(2\lambda - n)r_0} \right]^{1/2}. \quad (4)$$

Revival and fractional revivals appear during the time evolution of a suitably prepared wave packet and are well studied in the literature [6–8]. Here we study the effect of decoherence on the motion of a molecular wave packet through its sub-Planck scale structures. These structures are found at one eighth of the fractional revival time in the Wigner phase space distribution [23]. The initial wave packet is taken here as SU(1,1) coherent state (CS) of this potential [39], which is obtained upon applying the displacement operator on the ground state. The CS is given by

$$\begin{aligned} |\eta, s\rangle &= e^{\alpha K_+ - \alpha^* K_-} |0, s\rangle \\ &= (1 - |\eta|^2)^{(1+s)/2} \sum_{k=0}^{\infty} \left[\frac{\Gamma(k+s+1)}{k! \Gamma(1+s)} \right]^{1/2} \eta^k |k, s\rangle, \end{aligned} \quad (5)$$

where $0 \leq k \leq [\lambda - 1/2]$ correspond to the bound states of the Morse potential and $k > [\lambda - 1/2]$ are the appropriate scattering states. The parameter η is associated with the ‘‘amplitude’’ of the CS and possesses the same phase of the displacement amplitude α , while its modulus is given by the relation $|\eta| = \tanh|\alpha|$ [39]. In our numerical analysis, we will always consider low energy coherent states well below the dissociation limit so that only the bound states of the Morse potential can be used as basis set.

III. MASTER EQUATION FOR THE MORSE OSCILLATOR

As described in Sec. I, we now investigate the effect of the decoherence of an external phononic or photonic environment on the sub-Planck scale structure. Therefore, the total model Hamiltonian is [29]

$$H = H_{\text{sys}} + H_E + H_I, \quad (6)$$

where H_{sys} is the Morse Hamiltonian of the vibrational mode, H_E is the environment Hamiltonian described by a set of independent bosonic modes,

$$H_E = \sum_k \hbar \omega_k (a_k^\dagger a_k + 1/2), \quad (7)$$

and H_I is the interaction between the Morse particle and the environment, which we choose of the following form (see also [32,40]):

$$H_I = \hbar \hat{O}^\dagger \sum_k \sigma_k a_k + \text{H.c.}, \quad (8)$$

where σ_k are coupling constants. This choice corresponds to assume the rotating wave approximation (RWA) in the interaction with the environment so that we neglect counter-rotating terms, while the operator \hat{O} is a generic operator of the vibrational mode, whose specific form depends on the considered environment. Using standard techniques [29], one gets in the usual Born-Markovian approximation, the following master equation for the reduced density operator of the Morse oscillator ρ ,

$$\begin{aligned} \frac{d}{dt} \rho = & -\frac{i}{\hbar} [H_{\text{sys}}, \rho] + [\hat{O}_2 \rho \hat{O}_1^\dagger + \hat{O} \rho \hat{O}_2^\dagger - \hat{O}^\dagger \hat{O}_2 \rho - \rho \hat{O}_2^\dagger \hat{O}] \\ & + [\hat{O}_1^\dagger \rho \hat{O} + \hat{O}^\dagger \rho \hat{O}_1 - \hat{O} \hat{O}_1^\dagger \rho - \rho \hat{O}_1 \hat{O}^\dagger], \end{aligned} \quad (9)$$

where the operators $\hat{O}_j (j=1,2)$ are new operators of the vibrational mode corresponding to ‘‘modifications’’ of the operator associated to the absorption from the environment (\hat{O}_1) or emission into the environment (\hat{O}_2) of vibrational quanta. This fact is easily understood if we look at their expression in the energy eigenbasis $|n, s\rangle$ used in Eq. (5). In fact, one has

$$\hat{O}_j = \sum_{m,n} O_j^{m,n} |m, s\rangle \langle n, s|, \quad (10)$$

where

$$O_1^{m,n} = O^{m,n} \pi g(\omega_{mn}) |\sigma(\omega_{mn})|^2 \bar{n}(\omega_{mn}), \quad (11)$$

$$O_2^{m,n} = O^{m,n} \pi g(\omega_{mn}) |\sigma(\omega_{mn})|^2 [\bar{n}(\omega_{mn}) + 1]. \quad (12)$$

The quantities $O^{m,n}$ are the matrix elements of \hat{O} , $g(\omega_{mn})$ is the density of states at the transition frequency between two energy levels, $\omega_{mn} = (E_m - E_n)/\hbar$, and $\bar{n}(\omega_{mn}) = [\exp\{\hbar \omega_{mn}/k_B T\} - 1]^{-1}$ is the mean thermal number of environmental excitations, being the latter at equilibrium at temperature T . The appearance of these two operators is a direct consequence of the nonlinearity of the molecular vibrational motion. In fact, in the linear case the transition frequencies ω_{mn} do not depend on n and m and therefore \hat{O}_1 and \hat{O}_2 become proportional to \hat{O} . As a consequence, master equation (9) becomes identical to the master equation of a harmonic oscillator in a thermal environment in the RWA [29].

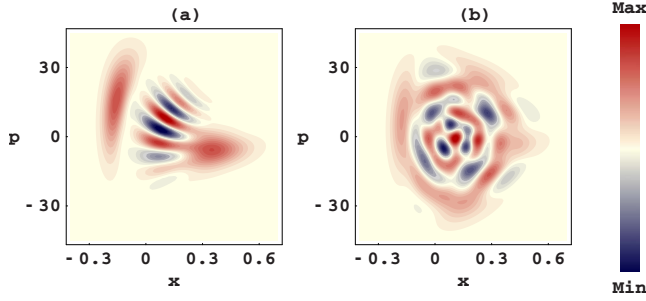


FIG. 1. (Color online) Time evolution of Morse wave packet in phase space Wigner distribution: (a) cat state at time $t = \frac{1}{4}T_{rev}$ and (b) sub-Planck scale structures, appeared at the middle at time $t = \frac{1}{8}T_{rev}$, where $\alpha=0.3$, $\beta=2.07932$, $r_0=3.04159$ a.u., and $\bar{n}=4$. Here, x and p are the dimensionless position and momentum variables, where $x=r/r_0-1$ and p is the corresponding scaled variable.

IV. SUB-PLANCK SCALE STRUCTURE AND ITS SENSITIVITY THROUGH DECOHERENCE

We now solve the master equation (9) for the specific case of the HI molecule and we adopt the Wigner function picture in order to look at the effects of decoherence on sub-Planck scale structures in phase space. The Wigner distribution is defined ($\hbar=1$) by

$$W(x,p,t) = \frac{r_0}{2\pi} \int_{-\infty}^{\infty} \left\langle x - \frac{x'}{2} \left| \rho(t) \right| x + \frac{x'}{2} \right\rangle e^{ix'p} dx' \quad (13)$$

and well describes the nonclassical interference effects associated with the time evolution of a wave packet in the nonlinear potential of the Morse oscillator.

This fact is visible, for example, in Fig. 1, which shows the time evolution of an initial CS wave packet in phase space at two different fractional revival times in the absence of decoherence. We have considered a HI molecule, which

has 30 bound states, with $\beta=2.0793$, reduced mass $\mu=1819.99$ a.u., $r_0=3.0416$ a.u., and $D=0.1125$ a.u. [23]. We have assumed here (and also in the following) that the initial wave packet is well below the dissociation limit, so that it involves only the lower levels of HI molecule (the energy distribution is peaked around the $\bar{n}=4$ vibrational level). Figure 1(a) shows the vibrational cat state after one fourth of the fractional revival time. Here, the revival time is $T_{rev}=4.89 \times 10^4$ a.u. Due to the anharmonicity of the system, one can notice the different squeezing effects in the two separated CSs forming the cat state. The number of ripples in the interference region increases for increasing mean energy of the initial CS. The sub-Planck scale structures appear in the interference region at one eighth of the fractional revival time [Fig. 1(b)], where one has a coherent superposition of four well distinct states, forming a so-called compass state [15]. For this reason we shall focus our attention on the effect of decoherence at this fractional revival time.

In the case of a molecular vibration, a bosonic environment well describes either the coupling via the dipole interaction with the outside electromagnetic field or, in the case of a molecule immersed in a liquid or gas, the coupling with the acoustic modes of the solvent. In both cases the operator \hat{O} is connected with the position operator of our Morse oscillator. In fact, \hat{O} describes the upper triangular part (in the energy basis representation) of the dipole moment operator of the molecule in the electromagnetic case and of the vibrational coordinate x in the acoustic phonon bath case. However the two situations are analogous because the dipole moment operator is proportional to x . Both environments are super-Ohmic, that is, we have

$$2\pi\sigma^2(\omega)g(\omega) = \delta\omega^3, \quad (14)$$

with δ characterizing the strength of the system-environment coupling. The physical meaning of the parameter δ can be

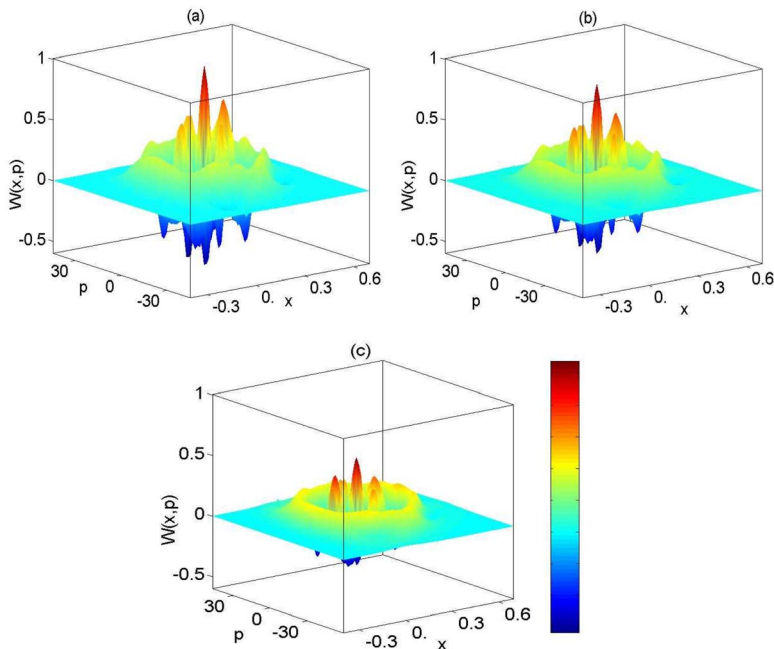


FIG. 2. (Color online) Wigner function of the coherent state at one eighth of revival time, approximately equal to a compass state, for three different values of the decoherence parameter δ : (a) $\delta=0$; (b) $\delta=0.54 \times 10^3$ a.u.; and (c) $\delta=2.2 \times 10^3$ a.u. Here, x and p are the dimensionless position and momentum variables, where $x=r/r_0-1$ and p is the corresponding scaled variable. The environment temperature is fixed at $T=10\hbar\omega_{01}/k_B$.

seen from the fact that the master equation (9) implies that the relaxation rate from level i to level j , Γ_{ij} at zero temperature is given by

$$\Gamma_{ij} = \delta r_{ij}^2 \omega_{ij}^3, \quad (15)$$

where r_{ij} is the corresponding matrix element of the position operator between the two vibrational levels. Here we have chosen the coupling constant δ such that the ratio Γ_{01}/ω_{01} ranges from 0.5×10^{-5} to 12.5×10^{-5} . These values correspond to reasonable values of the coupling constant δ ; in fact, considering a typical electric dipole moment of a diatomic molecule one gets $\delta \approx 10^{-12} \text{ m}^{-2} \text{ s}^2 = 4.78 \text{ a.u.}$ for the case of an electromagnetic environment. Instead, considering a dilute solvent one gets $\delta \approx 2 \times 10^{-11} \text{ m}^{-2} \text{ s}^2 = 95.66 \text{ a.u.}$ for the case of a phononic environment. One should note that position variable in our study is a dimensionless quantity (scaled by r_0). Hence, in the case of an electromagnetic environment, the order of δ in our case would be $\delta = 4.37 \times 10^3 \text{ a.u.}$, which is consistent with our study (see Fig. 3). Moreover, the temperature of the environment is kept fixed at $T = 10\hbar\omega_{01}/k_B$. Figure 2 shows the Wigner distribution at one eighth of the fractional revival time for different values of the coupling with the bosonic environment. Figure 2(a) refers to no decoherence ($\delta=0$) and therefore corresponds to Fig. 1(b). Figure 2(b) instead corresponds to $\delta=0.54 \times 10^3 \text{ a.u.}$ and Fig. 2(c) corresponds to a stronger decoherence, $\delta=2.2 \times 10^3 \text{ a.u.}$ One can clearly see that by increasing the coupling with the bosonic environment, the interference region is more and more affected.

As for the harmonic oscillator case [15,20], decoherence affects the structure as a whole; also here for the Morse oscillator, the sub-Planck structures due to quantum interference are more affected than the individual isolated coherent state components. In fact, a distinct difference can be observed in the decay rate of the amplitude of the sub-Planck scale structures and of the individual CSs. This is quantitatively shown in Fig. 3, where these decay rates are plotted versus the decoherence strength δ . We consider the left and right peaks of the CSs at $p=0$ and a negative peak at $x=0.077$ and $p=-6.064$, appearing in the sub-Planck interference region. The plot shows that the sub-Planck scale structure, i.e., the central interference patterns (dashed line in Fig. 3), disappears earlier compared to the individual CSs, as it

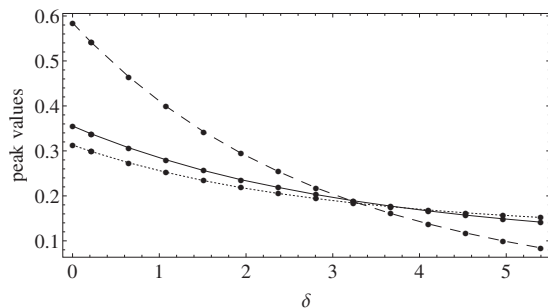


FIG. 3. Comparative variations between the left (dotted line) and right (solid line) peaks and the central negative sub-Planck region (dashed line) at $\frac{1}{8}T_{rev}$ with the coupling parameter δ (in unit of 10^3 a.u.). The environment temperature is $T = 10\hbar\omega_{01}/k_B$.

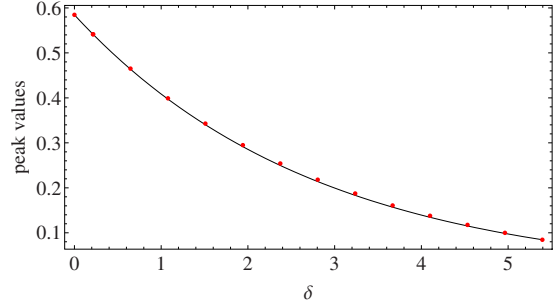


FIG. 4. (Color online) Variation in the central negative sub-Planck region at $\frac{1}{8}T_{rev}$ with the coupling parameter δ (in unit of 10^3 a.u.). Dots are the numerical data from our analysis. It satisfies an exponential law (solid line) $Ae^{-c\delta}$, with $A=0.5847$ and $c=0.3585$. The environment temperature is $T = 10\hbar\omega_{01}/k_B$.

happens in the harmonic case. It is possible to see that the decay of the amplitude of the sub-Planck structure follows very well an exponential law as a function of the decoherence strength δ , as expected in usual bosonic environments [28]. We find that a linear exponential function $Ae^{-c\delta}$ well fits with our results, with $A=0.5847$ and $c=0.3585$. Figure 4 shows how the rate of amplitude damping of the chosen negative interference region (i.e., sub-Planck region) matches with the exponential form.

It is now worth seeing the effect of environment temperature on decoherence for a fixed value of the coupling constant δ . Owing to Eqs. (11) and (12), one expects a Bose-Einstein dependence on temperature of the decay of the interference structures associated with sub-Planck structures, $a \exp\{-b/[e^{T_c/T}-1]\}$, where T_c corresponds to an effective transition temperature below which the discrete structure of the energy levels of the Morse oscillator starts to manifest itself. This is confirmed by Fig. 5, where the numerical results for the value of the negative peak are plotted versus temperature. The data, corresponding to $\delta=0.54 \times 10^3 \text{ a.u.}$, are well fitted by the above curve and the optimal fitting parameters are $a=0.5799$, $b=0.0127$, and $T_c=0.6688$. The data follow an exponential decay for $T/T_c \gg 1$, while the deviation from the exponential law (associated with the Bose-Einstein distribution dependence) is clearly visible only at very low temperatures, $T < T_c$, in the magnified view in the inset of Fig. 5.

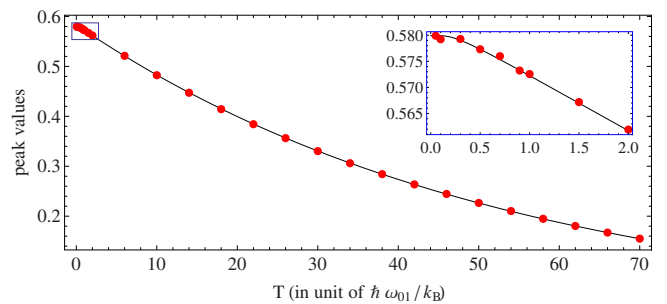


FIG. 5. (Color online) Variation in the central negative sub-Planck region at time $\frac{1}{8}T_{rev}$ with the environment temperature T in the case $\delta=0.54 \times 10^3 \text{ a.u.}$ It follows a Bose-distribution law, $a \exp\{-b/[e^{T_c/T}-1]\}$, for $a=0.5799$ and $b=0.0127$. Inset of the figure shows the variation near the critical temperature ($T_c=0.6688$).

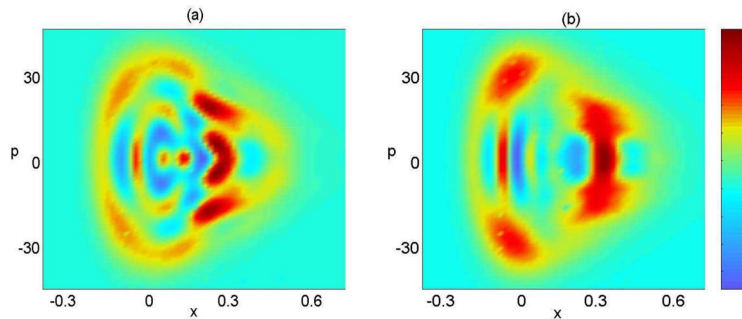


FIG. 6. (Color online) Wigner distribution at times (a) $\frac{3}{8}T_{rev}$ and (b) $\frac{5}{8}T_{rev}$, with coupling parameter $\delta=0.72 \times 10^3$ a.u and temperature $T=10\hbar\omega_{01}/k_B$. Central interference region in (a) (sub-Planck scale structure) disappears at a later time in (b). Here, x and p are the dimensionless position and momentum variables, where $x=r/r_0-1$ and p is the corresponding scaled variable.

So far we have been studying the decoherence effect on the sub-Planck scale structures at $1/8$ fractional revival time. Hence, it is a natural question to ask what happens at larger times when one can also obtain sub-Planck scale structures in the interference region of four-way breakup of a coherent state. Thus, we extend our study to the four-way breakup or the decoherence through sub-Planck scale regions at $3/8$ and $5/8$ fractional revival times. One expects a larger influence of decoherence on the sub-Planck structures for increasing times and this is confirmed by Fig. 6. Interference fringes in phase space are still visible at $3/8$ fractional revival time, while in Fig. 6(b), corresponding to $5/8$ fractional revival time, one can see that the sub-Planck structures completely disappear due to the larger decoherence effect, whereas the individual coherent states remain almost intact. The environment temperature is kept constant at $T=10\hbar\omega_{01}/k_B$, the coupling constant being $\delta=0.72 \times 10^3$ a.u.

V. CONCLUSIONS

We have investigated the time evolution of a coherent state wave packet in the Morse potential under the influence of a bosonic environment describing either photonic or phononic excitations. We have studied the effect of decoherence on the sub-Planck structures in phase space by looking at the evolution of the Wigner distribution. As it happens for the harmonic case, sub-Planck scale structures come out as the most sensitive to decoherence. A quantitative analysis provides an exponential decay of the amplitude of the quantum interference structures as a function of the coupling with the environment, in agreement with usual predictions [28]. Influence of the environment temperature on the decoherence is also shown quantitatively. This is according to the Bose-distribution law. Longer time effect on the decoherence is shown for providing another way to see the sensitiveness of sub-Planck scale structures compare to their original counterparts.

-
- [1] D. Zhong and A. H. Zewail, *J. Phys. Chem. A* **102**, 4031 (1998); A. H. Zewail, *ibid.* **104**, 5660 (2000).
- [2] E. A. Shapiro, M. Spanner, and M. Y. Ivanov, *Phys. Rev. Lett.* **91**, 237901 (2003); K. F. Lee, D. M. Villeneuve, P. B. Corkum, and E. A. Shapiro, *ibid.* **93**, 233601 (2004); D. Babikov, *J. Chem. Phys.* **121**, 7577 (2004).
- [3] B. M. Garraway and K.-A. Suominen, *Contemp. Phys.* **43**, 97 (2002).
- [4] M. Gruebele and A. H. Zewail, *J. Chem. Phys.* **98**, 883 (1993); M. J. J. Vrakking, D. M. Villeneuve, and A. Stolow, *Phys. Rev. A* **54**, R37 (1996).
- [5] P. M. Morse, *Phys. Rev.* **34**, 57 (1929).
- [6] I. Sh. Averbukh and N. F. Perelman, *Phys. Lett. A* **139**, 449 (1989).
- [7] R. Bluhm, V. A. Kostelecky, and J. Porter, *Am. J. Phys.* **64**, 944 (1996).
- [8] R. W. Robinett, *Phys. Rep.* **392**, 1 (2004), and references therein.
- [9] H. Katsuki *et al.*, *Science* **311**, 1589 (2006).
- [10] K. E. Cahill and R. J. Glauber, *Phys. Rev.* **177**, 1882 (1969).
- [11] W. Schleich and J. A. Wheeler, *Nature (London)* **326**, 574 (1987); *J. Opt. Soc. Am. B* **4**, 1715 (1987); W. Schleich, D. F. Walls, and J. A. Wheeler, *Phys. Rev. A* **38**, 1177 (1988); W. P. Schleich, *Quantum Optics in Phase Space* (Wiley-VCH, Berlin, 2001), and references therein.
- [12] W. Vogel, *Phys. Rev. Lett.* **84**, 1849 (2000).
- [13] Th. Richter and W. Vogel, *Phys. Rev. Lett.* **89**, 283601 (2002).
- [14] P. Földi, A. Czirják, B. Molnár, and M. G. Benedict, *Opt. Express* **10**, 376 (2002).
- [15] W. H. Zurek, *Nature (London)* **412**, 712 (2001).
- [16] Ph. Jacquod, I. Adagideli, and C. W. J. Beenakker, *Phys. Rev. Lett.* **89**, 154103 (2002).
- [17] D. A. Wisniacki, *Phys. Rev. E* **67**, 016205 (2003).
- [18] G. S. Agarwal and P. K. Pathak, *Phys. Rev. A* **70**, 053813 (2004).
- [19] P. K. Pathak and G. S. Agarwal, *Phys. Rev. A* **71**, 043823 (2005).
- [20] F. Toscano, D. A. R. Dalvit, L. Davidovich, and W. H. Zurek, *Phys. Rev. A* **73**, 023803 (2006).
- [21] D. A. R. Dalvit, R. L. de M. Filho, and F. Toscano, *New J. Phys.* **8**, 276 (2006).
- [22] L. Praxmeyer, P. Wasylczyk, C. Radzewicz, and K. Wódkiewicz, *Phys. Rev. Lett.* **98**, 063901 (2007).
- [23] S. Ghosh, A. Chiruvelli, J. Banerji, and P. K. Panigrahi, *Phys. Rev. A* **73**, 013411 (2006).
- [24] J. R. Bhatt, P. K. Panigrahi, and M. Vyas, *Phys. Rev. A* **78**, 034101 (2008).
- [25] M. Stobinska, G. J. Milburn, and K. Wódkiewicz, *Phys. Rev. A*

- 78**, 013810 (2008).
- [26] J. Banerji, *Contemp. Phys.* **48**, 157 (2007).
- [27] A. J. Scott and S. M. Caves, *Ann. Phys.* **323**, 2685 (2008).
- [28] W. H. Zurek, *Rev. Mod. Phys.* **75**, 715 (2003).
- [29] C. W. Gardiner and P. Zoller, *Quantum Noise* (Springer, Berlin, 1991).
- [30] D. Giulini, E. Joos, C. Kiefer, J. Kupsch, I.-O. Stamatescu, and H. D. Zeh, *Decoherence and the Appearance of a Classical World in Quantum Theory* (Springer, Berlin, 1996).
- [31] C. Brif, H. Rabitz, S. Wallentowitz, and I. A. Walmsley, *Phys. Rev. A* **63**, 063404 (2001).
- [32] P. Földi, M. G. Benedict, A. Czirják, and B. Molnár, *Phys. Rev. A* **67**, 032104 (2003).
- [33] S. I. Vetchinkin, A. S. Vetchinkin, V. V. Eryomin, and I. M. Umanskii, *Chem. Phys. Lett.* **215**, 11 (1993).
- [34] S. I. Vetchinkin and V. V. Eryomin, *Chem. Phys. Lett.* **222**, 394 (1994).
- [35] J. P. Dahl and M. Springborg, *J. Chem. Phys.* **88**, 4535 (1988).
- [36] A. Frank, A. L. Rivera, and K. B. Wolf, *Phys. Rev. A* **61**, 054102 (2000).
- [37] R. Graham and M. Höhnerbach, *Phys. Rev. A* **45**, 5078 (1992).
- [38] B. Molnár, P. Földi, M. G. Benedict, and F. Bartha, *Europhys. Lett.* **61**, 445 (2003).
- [39] S. Kais and R. D. Levine, *Phys. Rev. A* **41**, 2301 (1990).
- [40] Y. Elran and P. Brumer, *J. Chem. Phys.* **121**, 2673 (2004).